Highly crystalline anisotropic superstructures *via* magnetic field induced nanoparticle assembly†

Jong-Il Park,‡ Young-wook Jun, Jin-sil Choi and Jinwoo Cheon*

Received (in Cambridge, UK) 15th August 2007, Accepted 31st October 2007
First published as an Advance Article on the web 8th November 2007
DOI: 10.1039/b712513e

A magnetic field is successfully utilized to induce the fabrication of size controllable one-dimensional (1-D) supercrystals which are composed of a highly crystalline assembly of fcc-packed cobalt nanoparticles; the anisotropy associated supercrystal magnetism is enhanced with four times higher coercivity than that of randomly aggregated nanoparticles.

Recent synthetic advances of nanomaterials have enabled the development of various nanoparticle building blocks with distinct morphologies and properties.[1] One of the important issues required for their applications in electronics and biomedical sciences is how to systematically assemble these building blocks into highly ordered superstructures. Various assembly techniques have been developed, which include solvent evaporation induced assembly,[2,3] Langmuir–Blodgett nanoparticle assembly,[4] and molecular linker induced assembly.[5] Most of these typically produce isotropic 0-dimensional (0-D) superstructures. On the other hand, the use of controllable external electric or magnetic fields is also an attractive option for the fabrication of nanoparticle superstructures due to its simplicity and effectiveness.[3,6–9] More importantly, this is advantageous for the fabrication of anisotropic 1-D superstructures, which can potentially provide unique properties arising from their anisotropic morphology. We here demonstrate the magnetically controlled fabrication of 1-D anisotropic supercrystals comprised of face centered cubic (fcc)-packed cobalt nanoparticles. By investigating magnetic field and nanoparticle concentration effects, it is possible to produce various anisotropic supercrystals with different sizes, shapes and aspect ratios. A strong shape-dependent anisotropy effect on the magnetism is also observed in supercrystal rods. Although the groups of Pileni,[7] Prasad,[8] and Murray[3] have already demonstrated the formation of 1-D structures, the obtained materials are either amorphously aggregated or limited to a simple wire shape. Our study uniquely demonstrates that the formation of highly crystalline 1-D superstructures with structural evolution from dots to rods and to wires is possible in a controlled manner.

Cobalt nanoparticles were synthesized using a literature method by injecting $Co_2(CO)_8$ into a refluxing toluene solution containing oleic acid and sodium bis(2-ethylhexyl) sulfosuccinate.[10] The obtained nanoparticles were ~10 nm spheres with high monodispersity (σ = ~8%). The nanoparticles were redispersed in nonane at a 2 mM concentration based on Co. Supercrystal rods were assembled through the following procedures. A portion (100 μl) of the nanoparticle solution was dropped on a 1 × 1 cm^2 Si substrate which was pre-positioned either perpendicularly or parallel to an external magnetic field direction generated by two parallel magnets and then the solvent was allowed to slowly evaporate (Fig. 1(a), Fig. 3(a)). The magnitude of the external magnetic field exerted on the nanoparticles was controlled by changing the inter-magnet distance.

Fig. 1(b) shows a low magnification transmission electron microscopic (TEM) image of nanoparticle superstructures assembled under an external magnetic field of 2400 Oe. Anisotropic rod-shaped supercrystals are observed with a size of ~130 nm in width and ~450 nm in length (aspect ratio: ~3.5). A higher magnification TEM image shows the detailed crystalline structure of the supercrystal rods (Fig. 1(c)). The supercrystal rods are well-ordered fcc-structured assemblies of cobalt nanoparticles. Fig. 1(d) shows the schematic unit cell structure of fcc packed supercrystals of cobalt nanoparticles. The capping ligand coated cobalt nanoparticle is approximately considered as a 12.8 nm sized hard sphere (10 nm (cobalt) + 2.8 nm (two monolayers of oleic acid)). A supercrystal rod corresponds with the $[001]_{SL}$ projection of the model-fcc structure (Fig. 1(c), (e)). An alternative view of the supercrystal rod is also observed, which corresponds to the $[\bar{1}11]_{SL}$

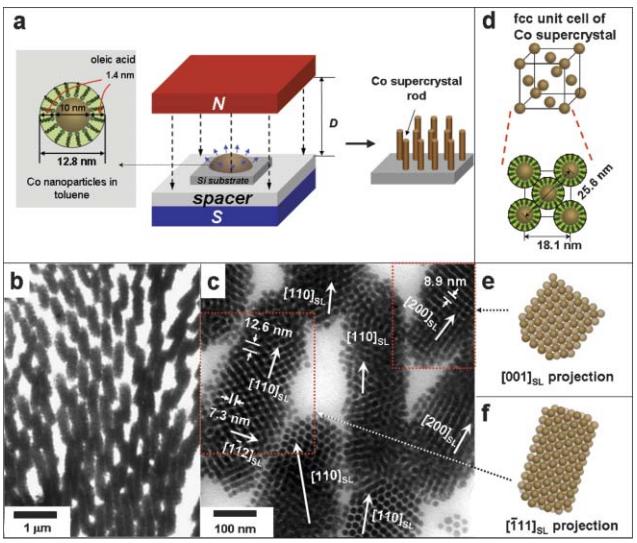

Fig. 1 (a) Schematic of Co supercrystal formation; (b) low and (c) high magnification TEM images; (d) unit cell structure; (e) $[001]_{SL}$ and (f) $[111]_{SL}$ projections of fcc-structured supercrystals.

Department of Chemistry and Nanomedical National Core Research Center (NCRC), Yonsei University, Seoul, 120-749, Korea. E-mail: jcheon@yonsei.ac.kr

† Electronic supplementary information (ESI) available: Small-angle XRD, magnetism and HRTEM analyses of supercrystals. See DOI: 10.1039/b712513e

‡ Current address: Research Institute of Industrial Science & Technology, Pohang, 790-330, Kyungbuk, Korea.

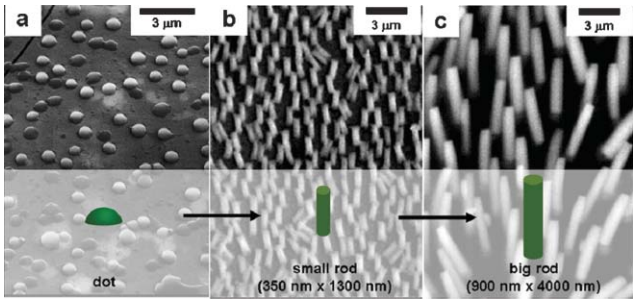

Fig. 2 Magnetic field and concentration effects on supercrystal formation. (a) Supercrystal dots obtained in the absence of external magnetic field. (b) and (c): Supercrystal rods obtained by evaporation of 10 mM (b) and 100 mM (c) Co nanoparticle solutions.

(SL: superlattice) projection of the fcc structure (Fig. 1(c), (f)). Our supercrystals have a periodicity of interplanar distances of 8.9 nm for $(100)_{SL}$, 7.3 nm for $(112)_{SL}$, and 12.6 nm for $(110)_{SL}$ (Fig. 1(c)). The measured lattice parameter from this TEM investigation is 17.8 nm which is further supported by small-angle X-ray diffraction (XRD) studies (see ESI†). This almost matches with the calculated lattice parameter of 18.1 nm of the fcc-model supercrystals. Our supercrystal rods are mainly elongated along a specific direction of $[110]_{SL}$ (*vide infra*).

The size and aspect ratio control of the supercrystals is possible by changing either the magnetic field or the initial concentration of nanoparticle solution. In the absence of the magnetic field, ~1 μm sized supercrystal dots are obtained (Fig. 2(a)). In contrast, when an external magnetic field is applied to the 2 mM cobalt nanoparticle solution, anisotropic supercrystal rods with the size of ~130 nm in width and ~450 nm in length result (Fig. 1(b)). At higher concentration of nanoparticle solution (10 mM), the size of supercrystal rods increases to ~350 nm in width and ~1300 nm in length with a similar aspect ratio, ~3.7 (Fig. 2(b)). At a concentration of 100 mM, monodispersed supercrystal rods with 900 nm width and 4000 nm length (aspect ratio: ~4.4) are obtained (Fig. 2(c)).

We further examined the effect of the external magnetic field direction. When the external magnetic field is applied to the substrate horizontally, elongated wire shapes of supercrystals with 300 nm diameter are observed, rather than rod-shapes (Fig. 3). Higher magnification TEM images show that the obtained supercrystal wires also have an fcc structure along the $[110]_{SL}$ direction.

Our anisotropic supercrystal rods exhibit unique magnetic behavior. The magnetism of the 0.9 × 4.0 μm^2 supercrystal rods was measured with a superconducting quantum interference device (SQUID) at 5 K. The supercrystal rods possess a significantly enhanced (four times) magnetic coercivity of 6400 Oe, compared to that of randomly aggregated cobalt nanoparticles (1600 Oe) (Fig. 4(a)). Such enhanced magnetism results from increased supercrystal shape anisotropy and dipole–dipole interaction between uni-directionally aligned nanoparticles (see ESI†).[7]

Fig. 4(b) shows schematic drawings of magnetic dipolar interactions between magnetic nanoparticles. Under an external magnetic field, a nanoparticle acquires a magnetic dipole, $m = \mu_0 \chi V H$, where μ_0 is the magnetic permeability of vacuum, χ is the magnetic susceptibility, and V is the volume of the nanoparticle.[10] This induces a magnetic dipole–dipole interaction (u) between two

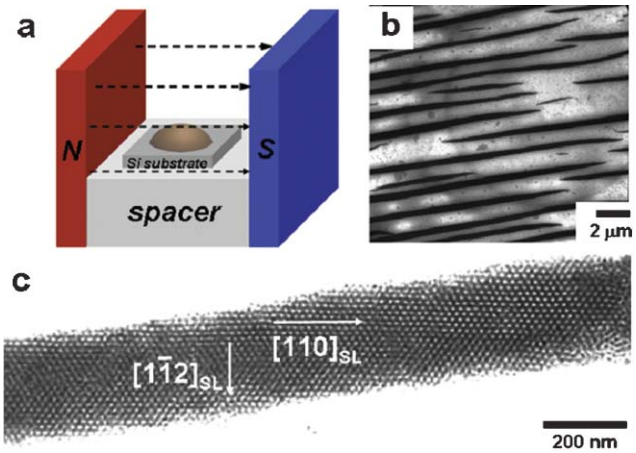

Fig. 3 Co supercrystal wires. (a) Schematic of experiments; (b) low and (c) high magnification TEM images.

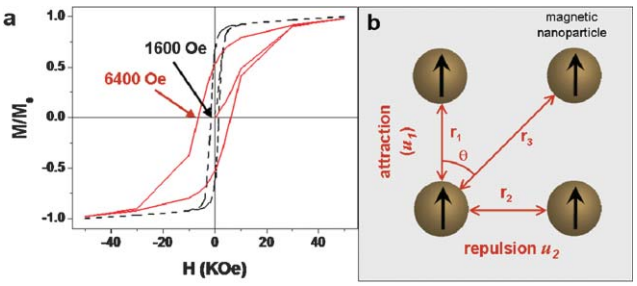

Fig. 4 (a) Enhanced magnetism of Co supercrystal rods (red solid line) compared to that of randomly aggregated nanoparticles (black dashed line). (b) Schematic of magnetic dipole interaction between nanoparticles.

nanoparticles separated by r, with an angle θ between r and m, $u(r, \theta) = -(m^2/4\pi\mu_0 r^3)(3\cos^2\theta - 1)$.[11] Two nanoparticles separated from each other with a distance of r_1 and $\theta = 0$ interact attractively ($u_1 = -2m^2/4\pi\mu_0 r_1^3$). In contrast, two nanoparticles at a distance of r_2 and $\theta = \pi/2$ repel each other due to a repulsive interaction, $u_2 = m^2/4\pi\mu_0 r_2^2$. At the initial stage of nanoparticle assembly, such dipolar interaction is very weak. However, as the solvent evaporates, the dipolar interaction energy becomes significant. Due to attractive dipolar interaction between nanoparticles aligned through the external field direction and repulsive interactions along the direction perpendicular to the field axis, anisotropic growth of nanoparticle supercrystals along the external magnetic field direction is facilitated. In our case, relatively thick 1-D shaped fcc-packed supercrystals are preferred rather than single chain structures, since the dipolar energy per particle in the fcc lattice is lower than that in a single chain structure.[11] In addition, the preferential growth of supercrystal rods and wires along the $[110]_{SL}$ direction results from the maximum dipole–dipole attraction along the $[110]_{SL}$ direction having a minimized r_1.

In summary, we have demonstrated magnetic field induced assembly of nanoparticles into crystalline anisotropic rods and wires. Controlling the magnetic field strength, nanoparticle concentration, and field direction yields various sizes and shapes of anisotropic supercrystals. Their enhanced magnetism due to the anisotropy has been also observed. Such anisotropic magnetic supercrystals can potentially be applicable as high-performance

integrated magnetic systems such as high-density magnetic storage devices and magnetic sensors.

This work is supported in part by the National Research Laboratory (R09-2006-000-10255-1) and BK21.

Notes and references

1 D. L. Klein, R. Roth, A. K. L. Lim, A. P. Alivisatos and P. L. McEuen, *Nature*, 1997, **389**, 699; N. L. Rosi and C. A. Mirkin, *Chem. Rev.*, 2005, **105**, 1547; Y. Jun, J. Choi and J. Cheon, *Angew. Chem., Int. Ed.*, 2006, **45**, 3414; Y. Yin and A. P. Alivisatos, *Nature*, 2005, **437**, 664.

2 R. L. Whetten, M. N. Shafigullin, J. T. Khoury, T. G. Schaaff, I. Vezmar, M. M. Alvarez and A. Wilkinson, *Acc. Chem. Res.*, 1999, **32**, 397; C. J. Kiely, J. Fink, M. Brust, D. Bethell and D. J. Schiffrin, *Nature*, 1998, **396**, 444; C. B. Murray, C. R. Kagan and M. G. Bawendi, *Science*, 1995, **270**, 1335; E. V. Shevchenko, D. V. Talapin, N. A. Kotov, S. O'Brien and C. B. Murray, *Nature*, 2006, **439**, 55; J. Cheon, J.-I. Park, J. Choi, Y. Jun, S. Kim, M. G. Kim, Y.-M. Kim and Y. J. Kim, *Proc. Natl. Acad. Sci. USA*, 2006, **103**, 3023.

3 C. B. Muarry, S. H. Sun, H. Doyle and T. Betley, *MRS Bull.*, 2001, **26**, 985.

4 F. Kim, S. Kwan, J. Akana and P. Yang, *J. Am. Chem. Soc.*, 2001, **123**, 4360; D. Whang, S. Jin, Y. Wu and C. M. Lieber, *Nano Lett.*, 2003, **3**, 1255; K. M. Gattas-Asfura, C. A. Constantine, M. J. Lynn, D. A. Thimann, X. Ji and R. M. Leblanc, *J. Am. Chem. Soc.*, 2005, **127**, 14640; S. Kwan, F. Kim, J. Akana and P. Yang, *Chem. Commun.*, 2001, 447.

5 C. A. Mirkin, R. L. Letsinger, R. C. Mucic and J. J. Storhoff, *Nature*, 1996, **382**, 607; A. P. Alivisatos, X. Peng, T. E. Wilson, K. P. Johnsson, C. J. Loweth, M. P. Bruchez, Jr. and P. G. Schultz, *Nature*, 1996, **382**, 609; M. D. Musick, C. D. Keating, L. A. Lyon, S. L. Botsko, D. J. Pena, W. D. Holliway, T. M. McEvoy, J. N. Richardson and M. J. Natan, *Chem. Mater.*, 2000, **12**, 2869.

6 S. Gupta, Q. Zhang, T. Emrick and T. P. Russell, *Nano Lett.*, 2006, **6**, 2066; K. M. Ryan, A. Mastroianni, K. A. Stancil, H. Liu and A. P. Alivisatos, *Nano Lett.*, 2006, **6**, 1479.

7 M. P. Pileni, *Adv. Funct. Mater.*, 2001, **11**, 323; Y. Lalatonne, J. Richardi and M. P. Pileni, *Nat. Mater.*, 2004, **3**, 121; M. P. Pileni, *Acc. Chem. Res.*, 2007, **40**, 685.

8 Y. Sahoo, M. Cheon, S. Wang, H. Luo, E. P. Furlani and P. N. Prasad, *J. Phys. Chem. B*, 2004, **108**, 3380.

9 M. Giersig and M. Hilgendorff, *J. Phys. D*, 1999, **32**, L111; M. Hilgendorff, B. Tesche and M. Giersig, *Aust. J. Chem.*, 2001, **54**, 497; G. Leo, Y. Chushkin, S. Luby, E. Majkova, I. Kostic, M. Ulmeanu, A. Luches, M. Giersig and M. Hilgendorff, *Mater. Sci. Eng. C*, 2003, **23**, 949.

10 J.-I. Park, N.-J. Kang, Y. Jun, S. J. Oh, H. C. Ri and J. Cheon, *ChemPhysChem*, 2002, **3**, 543.

11 H. Frohlich, in *Theory of Dielectrics: Dielectric Constants and Dielectric Loss*, Clarendon Press, Oxford, 1986.